JOURNAL OF AGRICULTURAL AND FOOD CHEMISTRY
ARTICLE

J. Agric. Food Chem. **2010,** *58,* 1189–1201 **1189**
DOI:10.1021/jf902939q

Cloning, Sequencing, Purification, and Crystal Structure of Grenache (*Vitis vinifera*) Polyphenol Oxidase

Victoria M. Virador,[†,⊗] Juan P. Reyes Grajeda,[‡,⊗] Alejandro Blanco-Labra,[§,⊗] Elizabeth Mendiola-Olaya,[§] Gary M. Smith,*[,∥] Abel Moreno,[⊥] and John R. Whitaker[∥]

[†]BG 10 RM 12C206, MSC 1906. National Institutes of Health, Bethesda, Maryland 20892, [‡]Instituto Nacional de Medicina Genómica, Dr. L. Orozco Periférico Sur 4124, Torre Zafiro II, 6° piso, Col. Jardínes del Pedregal, México, DF, CP 01900, México, [§]Centro de Investigación y de Estudios Avanzados del Instituto Politécnico Nacional Unidad Irapuato Libramiento Norte Km 9.6 carretera, Irapuato-León, Irapuato, Gto C.P. 36821 México, [∥]Department of Food Science and Technology, University of California, Davis, California 95616, and [⊥]Instituto de Química, Universidad Nacional Autónoma de México, México, D.F. 04510 Mexico. [⊗]These authors contributed equally to the research.

The full-length cDNA sequence (P93622_VITVI) of polyphenol oxidase (PPO) cDNA from grape *Vitis vinifera* L., cv Grenache, was found to encode a translated protein of 607 amino acids with an expected molecular weight of ca. 67 kDa and a predicted pI of 6.83. The translated amino acid sequence was 99%, identical to that of a white grape berry PPO (*1*) (5 out of 607 amino acid potential sequence differences). The protein was purified from Grenache grape berries by using traditional methods, and it was crystallized with ammonium acetate by the hanging-drop vapor diffusion method. The crystals were orthorhombic, space group $C222_1$. The structure was obtained at 2.2 Å resolution using synchrotron radiation using the 39 kDa isozyme of sweet potato PPO (PDB code: 1BT1) as a phase donor. The basic symmetry of the cell parameters (*a*, *b*, and *c* and α, β, and γ) as well as in the number of asymmetric units in the unit cell of the crystals of PPO, differed between the two proteins. The structures of the two enzymes are quite similar in overall fold, the location of the helix bundles at the core, and the active site in which three histidines bind each of the two catalytic copper ions, and one of the histidines is engaged in a thioether linkage with a cysteine residue. The possibility that the formation of the Cys-His thioether linkage constitutes the activation step is proposed. No evidence of phosphorylation or glycoslyation was found in the electron density map. The mass of the crystallized protein appears to be only 38.4 kDa, and the processing that occurs in the grape berry that leads to this smaller size is discussed.

KEYWORDS: Polyphenol oxidase; catechol oxidase; copper enzymes; *Vitis vinifera*; posttranslational processing; enzymatic browning; activation of proenzyme

Polyphenol oxidase (PPO; 1,2-benzenediol:oxygen oxidoreductase; EC 1.10.3.1) is a copper-containing enzyme that acts on a variety of substituted catechols. Polyphenol oxidases catalyze the oxidation of catechol and related phenolic compounds (reaction 1, **Scheme 1**, referred to as catechol oxidase or catecholase activity), but many also exhibit monophenol monooxygenase (EC 1.14.18.1) activity (reaction 2, **Scheme 1**, also referred to as cresolase or tyrosinase activity), catalyzing the oxidation of L-tyrosine to 3,4-dihydroxy-L-phenylalanine (L-DOPA). Cresolase activity is generally considered to be a property of fungal and mammalian enzymes, although it has also been observed in other organisms.

PPO is found in both prokaryotes and eukaryotes, and it is involved in the formation of pigments of polyphenolic origin such as melanins in animals, tannins in plants, and cuticles in arthropods (for a review, see ref *2*). Several plant PPO genes and cDNAs have been reported, including seven genes in tomato (*3*), several cDNAs from potato (*4*, *5*), and three cDNAs from fava bean (*6*). The existence of multiple genes and the localization of PPO in different plant compartments, together with its contribution to such diverse processes as wound response and ripening, have suggested the existence of multiple isozymes. In grape, only one PPO-encoding gene is indicated, based on Southern analysis (*1*). Most sequenced PPOs are encoded by *ca.* 2 kb transcripts and are single polypeptide enzymes, although mushroom PPO has four polypeptide subunits (*7*). Predicted molecular weights for mature monomeric plant PPOs range from 57 to 62 kDa (*3*, *4*). A 2 kb transcript is clearly capable of encoding a protein of more than 70 kDa, which is much larger than the PPOs that have been characterized; the initial gene product undergoes substantial processing (reviewed in ref *8*). The tomato leaf PPO gene encodes a 67 kDa protein containing an N-terminal signal peptide that targets the nuclear-encoded product to the thylakoid lumen. This precursor protein is hydrolytically

*Correspondence should be addressed to gmsmith@ucdavis.edu.

Published on Web 12/29/2009

Scheme 1

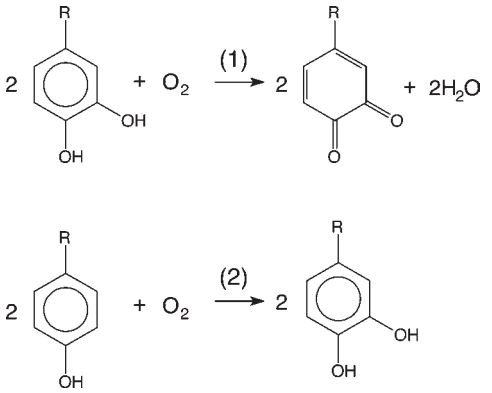

processed to a 62 kDa intermediate, which appears in the stroma, and is converted to the mature 59 kDa form following transport to the thylakoid lumen (*9*). Although this form is termed "mature", it is apparently not yet active.

The function of PPO has the characteristics of a wound or protective response in that it is activated by a disruption of tissue (*10*, *11*), as reviewed by Meyer (*12*) and, in at least some systems, becomes inactive after a limited number of catalytic cycles (*13*), thus restricting the location and amount of product to the region near the wound. Activation is thought to involve proteolytic processing that may cause release from the thylakoid membrane. Although proteolytic processing appears to be required for activity (*14*), many mature PPOs appear to remain in a latent form (reviewed in ref *8*).

Models for the reaction mechanism of PPO have been based on the *Neurospora* enzyme, which has an active site containing a binuclear copper center, with each copper ion ligated by three His residues (*15*−*17*). The crystal structure of the 39 kDa isozyme of sweet potato PPO shows a hydrophobic pocket close to the surface, which encloses the catalytic copper center located in a four-helix-bundle. H109, ligated to the CuA ion, is covalently linked to C92 by an unusual thioether bond (*18*), which had also been reported in *N. crasssa* PPO (*19*). There is a striking similarity between the active site of *N. crassa* PPO and that of the oxygen carrier hemocyanin from spiny lobster (*Panulirus interruptus*) (*20*). But despite the structural similarities, hemocyanin, tyrosinase, and catechol oxidase exhibit different reactivities.

In this work, the primary structure of grape PPO was deduced from cloned cDNA derived from the leaf RNA of a white variety of Grenache grapes (*Vitis vinifera* L. cv. Grenache). PPO was purified to homogeneity from Grenache berries. The protein produced 200 μm crystals, and the crystal structure of Grenache PPO was obtained at 2.2 Å resolution using synchrotron radiation by fitting the electron density to our cDNA sequence. We compare this structure to similar structures that are available and to the deduced amino acid sequence.

MATERIALS AND METHODS

Isolation of RNA and DNA. Young, actively growing leaf tissues of *V. vinifera* L. cv. Grenache were picked early in the morning. RNA was extracted by the method of Franke et al. (*21*), which is suitable for tissues that contain a high amount of polysaccharides and phenolic compounds. DNA was isolated by a modification of the method of Bowers et al. (*22*). Fresh leaf tissue (about 100 mg per tube) was ground in liquid nitrogen and added to 2 mL centrifuge tubes containing 1600 μL of extraction buffer composed of 0.1 M Tris HCl, pH 8.0, 1.4 M NaCl, 20 mM EDTA, 2% (w/v) CTAB, and 4 μL of 2-mercaptoethanol. Tubes were held at 60 °C for 15 min and then centrifuged for 2 min. DNA was precipitated from the supernatant with isopropanol/isoamyl alcohol (24:1; v/v). Pellets were washed in 70% (v/v) ethanol, dried under vacuum, resuspended in 300 μL of TE (10 mM Tris-HCl, 1 mM EDTA, pH 7.4), and heated to 60 °C for 1 h to dissolve. To precipitate the DNA, 200 μL of 5 M NaCl was added along with 1 mL of cold ethanol, and the sample was centrifuged at 4 °C for 5 min with a final wash in 70% (v/v) ethanol for 5 min. Pellets were dried under vacuum and resuspended in 100 μL of 0.1× TE (10 mM Tris-HCl, 0.1 mM EDTA, pH 8.0).

Table 1. Primers Used

cp1	$^{5'}$GGCTCGAGAGATCTGGATCCTTT$^{3'}$
cpt1	$^{5'}$CTCGAGAGATCTGGATCCTTTTTTTTTTTTTTTTTTT$^{3'}$
cp2	$^{5'}$GGCCACGCGTCGACTAGTAC$^{3'}$
cp2g	$^{5'}$GGCCACGCGTCGACTAGTACGGGIIGGGIIGGGIIG$^{3'}$
sp2	$^{5'}C_{1133}$AATGTCGATCGGATGTGGA$_{1152}{}^{3'}$
sp3	$^{5'}$TCCACATCCGATCGACATTG$^{3'}$
sp4	$^{5'}{}_{521}$ATAAAAAGGCCATTGAGCTGC$_{542}{}^{3'}$
sp5	$^{5'}$GCAGCTCAATGGCCTTTTTAT$^{3'}$
sp6	$^{5'}$CTCAATGGCCTTTTTATACT$^{3'}$
sp7	$^{5'}$AGCTATGGCTTCTTTGCCTTG$^{3'}$

Rapid Amplification of cDNA Ends (RACE-PCR). Specific primers (**Table 1**) were designed on the basis of a pileup of sequences from different PPOs (*2*). Total RNA (33 μg in 12.5 μL of H_2O) was heated for 3 min at 65 °C to denature the secondary structure. RACE-PCR was performed according to Frohman et al. (*23*). To obtain the 3′ end of Grenache leaf cDNA, the primers sp2 (**Table 1**) cp1 and cpt1 were utilized. PCR reactions were optimized according to Innis and Gelfand (*24*) with annealing steps 5 °C below the T_m of the particular pair of primers, resulting in clone pVM1. To obtain the 5′ end of Grenache leaf cDNA, 40 μg of total RNA was heated for 3 min at 65 °C to denature the secondary structure. Following the reverse transcriptase reaction, cDNAs were purified from unbound primers and unincorporated nucleotides by centrifugation at 4 °C in a Centricon 100 (Millipore, Billerica, MA) at 1000*g* for 20 min. For terminal tailing in a total volume of 20 μL, 15 μL of the purified cDNA pool was treated for 10 min at 37 °C, in 0.5× PCR buffer (50 mM KCl, 10 mM Tris-HCl, pH 9.0, 1% (v/v) Triton X-100), containing 0.1 mM dithiothreitol, 0.1 μg/μL BSA, 0.2 mM dCTP, and 20 units of terminal transferase (Promega, Madison, WI). Terminal transferase was heat inactivated at 70 °C after addition of 10 μL of 0.1 M EDTA and 70 μL of TE. For the second strand synthesis, 0.5−1 μL aliquots of the tailed RT products were added to a reaction containing, in a 25 mL total volume, 1× PCR buffer (50 mM KCl, 10 mM Tris-HCl, pH 9.0, 1% (v/v) Triton X-100), 0.1 mM each dNTP, 0.2 μM cp2g, 2 μM sp3, 2.5 mM $MgCl_2$, and 0.2 units of Taq polymerase (Promega, Madison, WI). After four PCR cycles with an annealing temperature of 45 °C for 30 s, the temperature was raised to 94 °C for 1 min. A 9:1 mix of primers cp2 and cp2g (4 μL of 10 μM stocks) was added along with 0.1 units of Taq polymerase, and PCR was continued for an additional 35 cycles with an annealing step of 57 °C. For nested amplification of fragments, 0.2−1 μL aliquots of these PCR products were amplified with primers sp3 and sp4 at 5 °C below the lowest T_m (*25*), to yield clone pVM2, or with nested primers sp5 and sp6 to yield clone pVM72.

Cloning, Sequencing, and Analysis of PPO PCR Products. The PCR products were separated using 1% submarine agarose electrophoresis preparative gels. DNA bands were eluted from the gel using a Gene Clean kit (MP Biomedicals, Solon, OH), ligated to pCRII (Invitrogen, Carlsbad, CA), and sequenced. The complete sequence reported here (GenBank accession number U83274), designated P93622_VITVI, was obtained by assembly and translation of the above-mentioned three overlapping cDNA fragments. BLASTp (*26*) was used to generate alignments.

Analytical Methods. Protein concentration was determined using the Bradford assay (*27*) or by following absorbance at 220 nm. PPO activity was determined by a modification of the colorimetric method described by Joslyn and Ponting (*28*) using 5 mM catechol as substrate and measuring the initial change in absorbance at 420 nm (pH 6.5, 25 °C). SDS-PAGE was carried out on slab gels containing 13% total acrylamide (electrophoresis supplies were from BioRad, Hercules, CA). The catecholase activity of PPO on slab gels after SDS-PAGE was determined using 4-*tert*-butylcatechol (Fluka, Buchs, Switzerland) as substrate. The substrate was readily oxidized to the corresponding yellow *o*-quinone, which in turn quickly reacted with the coupling agent, 4-amino-*N*,*N*-diethylaniline sulfate (Fluka, Buchs, Switzerland), to produce a deep blue adduct (*29*). The absence of tyrosinase (monophenolase) activity was confirmed by the method of Duckworth and Coleman (*30*), using tyrosine as substrate.

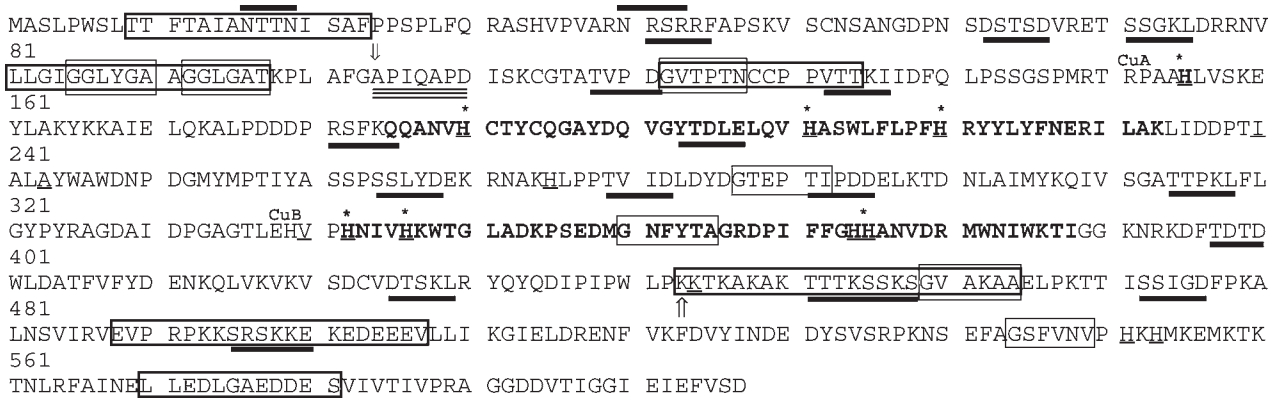

Figure 1. Deduced amino acid sequence of PPO from Grenache leaves, P93622_VITVI. Copper-binding regions, determined from homology to hemocyanins (Prosite http://www.expasy.ch), are in bold, ligand His residues are marked with an asterisk, His residues conserved across all higher plants are boldface and underlined, residues differing from those of the published ppo_vitvi sequence are underlined, and the first and last residues appearing in the X-ray structure are marked with down and up arrows, respectively. Predicted glycosylation sites are marked with an overbar, predicted phosphorylation sites are marked with a single underbar, predicted myrstolation sites are marked with a light box, and low complexity regions (*55*) are marked with a heavy box, as predicted by PROSITE (*56*). The three-line bar underline highlights sequence similarity to the N-terminal processing of spinach PPO: APILPDVEKC, which coincides with the first residue appearing in the X-ray structure.

Myosin (200,000 Da), β-galactosidase (116,250 Da), phosphorylase b (97,400 Da), bovine serum albumin (66,200 Da), ovalbumin (45,000 Da), carbonic anhydrase (31,000 Da), trypsin inhibitor (21,500 Da), lysozyme (14,400 Da), and aprotinin (6,500 Da) were used as molecular weight standards (all from Bio-Rad, Hercules, CA).

Purification of Grenache Polyphenol Oxidase. Mature Grenache grapes (200 g) were picked from the vineyard at the University of California, Davis, CA, and frozen. All procedures were carried out at 4 °C. Grapes were blended for 5 min with 2 volumes (w/v) of buffer (100 mM sodium phosphate, 0.03 M ascorbic acid, 10% (w/v) PVPP, pH 6.5). The pulp was separated by centrifugation (24000*g* for 30 min), and the supernatant, which contained little activity, was discarded. The precipitate was mixed with an equal volume of buffer (100 mM sodium phosphate, 0.1% (v/v) Triton X-100, 2.5% (w/v) PVPP at pH 6.5) and stirred for 30 min. After centrifugation (24000*g* for 30 min), the precipitate was discarded and the supernatant was concentrated by ultrafiltration using an YM10 membrane in an Amicon microconcentrator. The solution was brought to 40% saturation with ammonium sulfate, allowed to stand for 30 min, and centrifuged (39200*g* for 60 min). The supernatant was further saturated to 95% with ammonium sulfate, let stand for 30 min at 4 °C, and centrifuged (39200*g* for 60 min). The pellet (~50% of the total activity) was frozen until use. The precipitates from several extractions were dissolved in buffer (5 mM sodium phosphate, pH 8.0) and dialyzed against the same buffer at 4 °C. The sample was chromatographed on a Sephadex G-75 column. The fractions containing activity were pooled and subjected to anion exchange chromatography using an Econo-Pac Q cartridge (Bio-Rad). The protein eluting at ~0.1 M NaCl was applied to a Superose-R 12 column (Pharmacia HR10/30) equilibrated with 10 mM Tris-HCl, pH 7.5, and chromatographed in the same buffer, yielding one major peak with three shoulders, all of which contained activity. These fractions were analyzed by SDS PAGE and stained for protein (*31*) and activity by treatment with 25 mM 4-*tert*-butylcatechol and 25 mM 4-amino-*N*,*N*-diethylaniline sulfate. One peak showed a single protein and a single activity band and was selected for crystallization.

Crystallization of PPO. The enzyme was crystallized by using the hanging-drop vapor diffusion method in NEXTAL plates (Code NCP-24-100). Crystallization was achieved with Crystal Screen I (Hampton Research). The Hampton Research kit condition No. 9 produced useable crystals. Aliquots of 2.5 μL of freshly purified protein solution at a concentration of 10 mg/mL in 100 mM citrate buffer, pH 5.6, were mixed with the reservoir (2.5 μL) solution that had 30% (w/v) PEG-4000 in 100 mM buffer citrate pH 5.6 and 200 mM ammonium acetate. Crystallization boxes were incubated at 18 °C for 10 days. Between 1 week and 10 days, several crystals were obtained, reaching maximum dimensions of $0.20 \times 0.1 \times 0.1$ mm^3.

X-ray Diffraction and High-Resolution 3D Structure of Polyphenol Oxidase. X-ray data were collected at 2.2 Å resolution using synchrotron radiation in beamline X29 at the Brookhaven National Laboratory, Upton, NY. A full data set of 360 oscillation images half a degree each (360/0.5°) was collected at −165 °C with an ADSC Quantum Detector 315 with a crystal-detector distance of 300 mm. All data were integrated using CrystalClear and then reduced with SCALE and TRUNCATE of the CCP4 program (*32*).

Structure Determination and Refinement. The structure of native PPO was solved by the molecular replacement method (MOLREP) and refined by using suites CCP4 and CNS 1.1v. The phase donor molecule used for the replacement was the 39 kDa isozyme of sweet potato PPO (PDB code 1BT1), having a secondary structure identity of 56.8%. Electron density maps were created and adjusted by the Crystallographic Object-Oriented Toolkit (COOT) using the deduced primary structure. All data related to the structure were deposited in the PDB (code 2P3X).

RESULTS AND DISCUSSION

Cloning of Grenache Leaf Polyphenol Oxidase. Grenache PPO cDNA was cloned by the method of Frohman et al. (*23*). Rapid amplification of cDNA end (RACE) primers (**Table 1**) was based on two conserved regions of the amino acid sequences of several PPOs (*2*). Reverse transcriptase reactions employed RNA extracted from leaves and from immature grape berries; however, the first ca. 900 bp fragment that could be obtained by PCR originated from RNA from leaves, and all subsequent cloning attempts employed RT products from leaves. Primer pairs sp2 and cp1/cpt1 gave a 3′ end clone (clone pVM1). Clone pVM2 was derived by reamplification of 5′ end RACE products with primers sp3 and sp4, whereas clone pVM72 was derived from reamplification of 5′ end RACE products with primers sp7 and sp5/sp6. Three overlapping fragments were sequenced. Assembly of all three sequences produced the final sequence, P93622_VITVI (GenBank accession number U83274).

DNA Sequence Analysis of Grenache Leaf PPO. The complete Grenache PPO cDNA is 1978 bp long; it has a single ORF of 1824 bp and encodes a 607 amino acid product with a molecular weight of 67 kDa (Supporting Information Table 1). However, significant posttranslational processing is thought to occur to yield the mature, active protein, as discussed below.

Figure 1 shows the deduced amino acid sequence of Grenache leaf PPO, together with predicted sites of posttranslational modification. Possible phosphorylation sites are abundant, which is consistent with some reports on phosphorylation of PPOs; for example, Sokolenko et al. (*33*) suggested that a transmembrane

```
                1                                                    50
P93622_VITVI*  MASLPWSLTT FTAIANTTNI SAFPPSPLFQ RASHVPVARN RSRRFAPSKV
PPO_VITVI**    MASLPWSLTT STAIANTTNI SAFPPSPLFQ RASHVPVARN RSRRFAPSKV
PPO_MALDO      MTSLSPPVVT TPTVPNPA.. .TKPLSPFSQ NNSQVSLLTK PKRSFA.RKV
PPO_VICFA      MTSISasFIS TINVSSNSKI SHSSVYPFLQ KQHQSSKLRK PKR.....QV
PPO2_IPOBA     MASFTTSPCT SAAPKTPKSl sSATISSPLP KPSQI..HIA TAKRTHHFKV
PPOB_SOLTU     ...SSSSTTT IPLCTNKSLS SSFTtsSFLS KPSQLFLHGR RNQSF...KV
PPOA_SOLLC     MASLCSNSSS TSltSSTTCL SSTPT..... .ASQLFLHGK RNKTF...KV
PPO_SPIOL      MA.......T LSSPTIITTT SILLNNPFLP KTPQLSAHHH RGVRSVNGKV
PPOD_SOLLC     MASLCSNSST TSLKTPFTSL GSTP...... KPCQLFLHGK RNKAF...KV

                51                                                   100
P93622_VITVI   SCNSANGDPN SDSTSDVRET SSGKLDRRNV LLGIGGLYGA AGGLGATKPL
PPO_VITVI      SCNSANGDPN SDSTSDVRET SSGKLDRRNV LLGIGGLYGA AGGLGATKPL
PPO_MALDO      SCKATNNDQN DQAQS..... ...KLDRRNV LLGLGGLYGV AGM..GTDPF
PPO_VICFA      TCSSNNNQNN PKEEQELSNI VG...HRRNV LIGLGGIYGT L....ATNPS
PPO2_IPOBA     SCNAPNGD.. SQ........ .P.KLDRRDV LLGLGGLAGA ASLI--NNPL
PPOB_SOLTU     SCNANNNVGE HDKNLDT... ....VDRRNV LLGLGGLYGA AN....LAPL
PPOA_SOLLC     SCKVTNTNGN QDETNSV... .....DRRNV LLGLGGLYGV AN...AIPLA
PPO_SPIOL      SCQTKNNNGN DENNqnPNTN TPYLLDRRNI LLGLGGMYAA LGSEGANYYN
PPOD_SOLLC     SCKVTNTNGN QDETNSV... .....DRRNV LLGLGGLYGV AN...AIPLA

                101                                                  150
P93622_VITVI   AFGAPIQAPD ISKCGTATVP DGVTPTNCCP PVTTKIIDFQ LPSSGSPMRT
PPO_VITVI      AFGAPIQAPD ISKCGTATVP DGVTPTNCCP PVTTKIIDFQ LPSSGSPMRT
PPO_MALDO      AFAKPIAPPD VSKCGPADLP QGAVPTNCCP PPSTKIIDFK LPAP.AKLRI
PPO_VICFA      ALASPISPPD LSKCVPPslP SGTTPpnCCP PYSTKITDFK FPSN.QPLRV
PPO2_IPOBA     AFAEPIHAPE ISKCvpPklP PDAIVDNCCP PLATNVIPYK VPtSPSAMKI
PPOB_SOLTU     ASASPIPPPD LKSCGVAHVT EGVDVtsCCP PVPDDivPYY KFPPMTKLRI
PPOA_SOLLC     ASAAPTPPPD LSSCNKPKIN ATTepYFCCA PKPDDMSKVP yfPSVTKLRI
PPO_SPIOL      TLAAPI.LPD VEKCTLSdlW DGSVGDHCCP PpiTKDFEFk yHNHVKKVRR
PPOD_SOLLC     ASAAPTPPPD LSSCSIARID ENQVVssCCA PKPDDMEKVP yfPSMTKLRV

                151                                                  200
P93622_VITVI   RPAAHLVSKE YLAKYKKAIE LQKALPDDDP RSFKQQANVH CTYCQGAYDQ
PPO_VITVI      RPAAHLVSKE YLAKYKKAIE LQKALPDDDP RSFKQQANVH CTYCQGAYDQ
PPO_MALDO      RPPAHAVDQA YRDKYYKAME LMKALPDDDP RSFKQQAAVH CAYCDGAYDQ
PPO_VICFA      RQAAHLVDNE FLEKYKKATE LMKALPSNDP RNFTQQANIH CAYCDGAYSQ
PPO2_IPOBA     RPAIHRMDKE YIAKFEKAIR LMKELPADDP RNFYQQALVH CAYCNGGYVQ
PPOB_SOLTU     RPPAHAADEE YVAKYQLATS RMRELDKddP LGFKQQANIH CAYCNGAYKV
PPOA_SOLLC     RPPAHALDEA YIAKYNLAIS RMKDLDkdNP IGFKQQANIH CAYCNGGYSI
PPO_SPIOL      PAHKAYEDQE WLNDYKRAIA IMKSLPMSDP RSHMQQARVH CAYCDGSYPV
PPOD_SOLLC     RQPAHEADEE YIAKYNVSVT KMRDLDklNP IGFKQQANIH CAYCNGAYRI

                201                                                  250
P93622_VITVI   VGYTDLELQV HASWLFLPFH RYYLYFNERI LAKLIDDPTI ALAYWAWDNP
PPO_VITVI      VGYTDLELQV HASWLFLPFH RYYLYFNERI LAKLIDDPTF ALPYWAWDNP
PPO_MALDO      VGFPELELQI HNSWLFFPFH RYYLYFFEKI LGKLINDPTF ALPFWNWDSP
PPO_VICFA      IGFPDLKLQV HGSWLFFPFH RWYLYFYERI LGSLINDPTF ALPFWNYDAP
PPO2_IPOBA     TDYPDKEIQV HNSWLFFPFH RWYLYFYERI LGKLIGDPTF GLPFWNWDTP
PPOB_SOLTU     GGK...ELQV HFSWLFFPFH RWYLYFYERI LGSLINDPTF ALPYWNWDHP
PPOA_SOLLC     DGKV...LQV HNSWLFFPFH RWYLYFYERI LGSLIDDPTF GLPFWNWDHP
PPO_SPIOL      LGHNDTRLEV HASWLFPSFH RWYLYFYERI LGKLINKPDF ALPYWNWDHR
PPOD_SOLLC     GGK...ELQV HNSWLFFPFH RWYLYFYESN AGKLIDDPTF ALPYWNWDHP
```

Figure 2. Continued.

```
                251                                                 300
P93622_VITVI    DGMYMPTIYA SSPSSLYDEK RNAKHLPPTV IDLDYDGTEP TIPDDELKTD
PPO_VITVI       DGMYMPTIYA SSPSSLYDEK RNAKHLPPTV IDLDYDGTEP TIPDDELKTD
PPO_MALDO       AGMPLPAIYA DPKSPLYDKL RSANHQPPTL VDLDYNGTED NVSKETTINA
PPO_VICFA       DGMQLPTIYA DKASPLYDEL RNASHQPPTL IDLNFCDIGS DIDRNELIKT
PPO2_IPOBA      AGMLIPQYFR NQNSPLYDEN RNQSHLP-LV MDLGYAGTDT DVTDQERISN
PPOB_SOLTU      KGMRIPPMFD REGSSLYDDK RNQNHRNGTI IDLGHFGQEV DTPQLQIMTN
PPOA_SOLLC      KGMRFPPMFD VPGTALYDER RgqIHNGNG IDLGYFGDQV ETTQLQLMTN
PPO_SPIOL       DGMRIPEIFK EMDSPLFDPN RNTNHL.DKM MNLSFVSDEe dVNEDDQYEE
PPOD_SOLLC      KGMRFPAMYD REGTFLFDET RDQSHRNGTV IDLGFFGNEV ETTQLQMMSN

                301                                                 350
P93622_VITVI    NLAIMYKQIV SGATTPKLFL GYPYRAGDAI DPGAGTLEHV PHNIVHKWTG
PPO_VITVI       NLAIMYKQIV SGATTPKLFL GYPYRAGDAI DPGAGTLEHA PHNIVHKWTG
PPO_MALDO       NLKIMYRQMV SNSKNAKLFF GNPYRAGDEP DPGGGSIEGT PHAPVHLWTG
PPO_VICFA       NLSIMYRQVY SNGKTSRLFL GNPYRAGDAE PQGAGSIENV PHAPVHTWTG
PPO2_IPOBA      NLALMYKSMV TNAGTAELFL GKPYKAGdpV NKGGGSIENI PHTPVHRWVg
PPOB_SOLTU      NLTLMYRQMV TNAPCPSQFF GAAYPLGTEP SPGMGTIENI PHTPVHIWTG
PPOA_SOLLC      NLTLMYRQLV TNSPCPLMSL VDLTLFGSTV .EDAGTVENI PHSPVHIWVG
PPO_SPIOL       NILLMRKAMV YPSvkAELFL GSPYRAGDKM esGAGILERM PHNSVHVWTR
PPOD_SOLLC      NLTLMYRQMV TNAPCPRMFF GDLMISGITL .NSPGTIENI PHGPVHIWSG

                351                                                 400
P93622_VITVI    LADKPSEDMG NFYTAGRDPI FFGHHANVDR MWNIWKTIGG KNRKDFTDTD
PPO_VITVI       LADKPSEDMG NFYTAGRDPI FFGHHANVDR MWNIWKTIGG KNRKDFTDTD
PPO_MALDO       DNTQpfEDMG NFYSAGRDPI FFAHHSNVDR MWSIWKTLGG K.RTDLTDSD
PPO_VICFA       DNTQtiEDMG IFYSAARDPI FYSHHSNVDR LWYIWKTLGG K.KHDFTDKD
PPO2_IPOBA      pRTQNGEDMG NFYSAGRDIL FYCHHSNVDR MWTIWQQLGG KGRrdFTDSD
PPOB_SOLTU      DsqKNGENMG NFYSAGLDPI FYCHHANVDR MWDEWKLIGG K.RRDLSNKD
PPOA_SOLLC      TRRGsgEDMG NFYSAGLDPL FYCHHSNVDR MWNEWKATGG K.RTDIQNKD
PPO_SPIOL       SNtkGNQDMG AFWSAGRDPL FYCHHSNVDR MWSLWTdhGG NFPKTPEYDD
PPOD_SOLLC      TVRGsrGEYG HFYSAGLDPV FFCHHSNVDR MWSEWKATGG K.RTDITHKD

                401                                                 450
P93622_VITVI    WLDATFVFYD ENKQLVKVKV SDCVDTSKLR YQYQDIPIPW LPKKTKAKAK
PPO_VITVI       WLDATFVFYD ENKQLVKVKV SDCVDTSKLR YQYQDIPIPW LPKNTKAKAK
PPO_MALDO       WLDSGFLFYN ENAELVRVKV RDCLETKNLG YVYQDVDIPW LSSKprAKVA
PPO_VICFA       WLESGFLFYD ENKNLVRVNV KDSLDIDKLG YAYQDVPIPW EKAKPVPRRT
PPO2_IPOBA      WLDATFIFYD ENKQAVRVRV GDALDNQKLG YKYEFTNLPW L------NSK
PPOB_SOLTU      WLNSEFFFYD ENRNPYRVKV RDCLDSKKMG FSYAPMPTPW R......NFK
PPOA_SOLLC      WLNSEFFFYD ENGNPFKVRV RDCLDTKKMG YDYHATATPW R......NFK
PPO_SPIOL       YRNAYFYFYD ENANPVRVYV RDSFDTERLG YKYEDQELPW MSITQQQQQQ
PPOD_SOLLC      WLNSEFFFYD ENENPYRVKV RDCLDTKKMG YDYKPMRTPW R......NFK

                451                                                 500
P93622_VITVI    TTTKSSKSGV AKAAELPKTT ISSIGDFPKA LNSVIRVEVP RPKKSRSKKE
PPO_VITVI       TTTKSSKSGV AKAAELPKTT ISSIGDFPKA LNSVIRVEVP RPKKSRSKKE
PPO_MALDO       LSKVAKKLGV AHAAVASSSK VVAGTEFPIS LGSKISTVVK RPkkKRSKKA
PPO_VICFA       KVQKLVEVEV NDGNLRKSPT IFLVrtFPLV LNNKVSAIVK RPKKLRSKKE
PPO2_IPOBA      PLPTKKKTGL AARSKAPFVT ----DVFPLT LDKVVQVKVP RPKKSRSKEE
PPOB_SOLTU      PIRKTTAGKV NTASIAPVTK VFPLAKLDRA ISFSIT.... RPASSRTTQE
PPOA_SOLLC      PKTKASAGKV NTGSIPPESQ VFPLAKLDKA ISFSIN.... RPASSRTQQE
PPO_SPIOL       QRQQQRQPLL GGRLkvKKVL TELKVMLPLP LksVIKTKVD RPKKSRTKED
PPOD_SOLLC      PLTKASAGKV NTSSIPPVSQ AFPLAKLDKA VSFSIN.... RPTSSRTPQE
```

Figure 2. Continued.

```
                501                                                  550
P93622_VITVI    KEDEEEVLLI KGIELDRENF VKFDVYINDE DYSVSRPKNS EFAGSFVNVP
PPO_VITVI       KEDEEEVLLI KGIELDRENF VKFDVYINDE DYSVSRPKNS EFAGSFVNVP
PPO_MALDO       KEDEEEILVI EGIEFDRDVA VKFDVYVNDV DDLPSGPDKT EFAGSFVSVP
PPO_VICFA       KEEEEEVLVI EGIEFYMNIA IKFDVYINDE DDKVG.AGNT EFAGSFVNIP
PPO2_IPOBA      KEAEEEILEI QGIEVAIDQY AKFDVYLNDE DEPEAGKEKA EYAGSFAHLP
PPOB_SOLTU      KNEQEEILTF NKVAYDDTKY VRFDVFLNVD KtnADELDKA EFAGSYTSLP
PPOA_SOLLC      KNAQEEVLTF NAIKYDNRDY IRFDVFLNVD NnnANELDKA EFAGSYTSLP
PPO_SPIOL       KLEHEEVLVI NFKLGKSKDF IKFDVYINDG TDYKPEDknL EYAGSFTSLT
PPOD_SOLLC      KNAQEEMLTF NSIRYDNRGY IRFDVFLNVD NnnANELDKA EFAGSYTSLP

                551                                                  600
P93622_VITVI    HKHMKEMKTK TNLRFAINEL LEDLGAEDDE SVIVTIVPRA GGDDVTIGGI
PPO_VITVI       HKHMKEMKTK TNLRFAINEL LEDLGAEDDE SVIVTIVPRA GGDDVTIGGI
PPO_MALDO       HSHKHKKKMN TILRLGLTDL LEEIEAEDDD SVVVTLVPKF GA..VKIGGI
PPO2_IPOBA      HKHTGSKKIR TSLSLGLNEP LEDLGAEDDD AVLVTLAPKV GGGVVTVENI
PPO_VICFA       HSAhkNKKII TSLRLGITDL LEDLHVEGDD NIVVTLVPKC GSGQVKINNV
PPOB_SOLTU      HVHGNNTntS VTFKLAITEL LEDNGLEDED TIAVTLVPKV GGEGVSIESV
PPOA_SOLLC      HVHRVGDPKH ttLRLAITEL LEDIGLEDED TIAVTLVPKK G..DISIGGV
PPO_SPIOL       HGGgeDMGKN TVLKLALNQL LEDLDATDDD SIQVTIVPKS GTDSIVITGI
PPOD_SOLLC      HVHRAGETnt VDFQLAITEL LEDIGLEDED TIAVTLVPKR GGEGISIENA

                601  608
P93622_VITVI    EIEFVSD
PPO_VITVI       EIEFVSD.
PPO_MALDO       KIEFAS..
PPO_VICFA       EIVFE.D.
PPO2_IPOBA      KIVYGS
PPOB_SOLTU      EIKLE.DC
PPOA_SOLLC      EIKL....
PPO_SPIOL       DIE.....
PPOD_SOLLC      TISL.ADC
```

Figure 2. Multisequence alignment of PPOs. Alignment of amino acid sequences obtained from c-DNAs of 9 higher plant PPOs. (See text for details.) Conserved amino acids are shown with dashes. Gaps are dots. Upper case letters are aligned; lower case letters are insertions. Putative processing site, based on similarity with sequence APILPDVEKC, which was shown to be the N-terminal sequence of mature spinach PPO (*57*). The sequence alignment corresponds to PPOs from the following plants: P93622_VITVI (Grenache leaf cDNA), PPO_VITVI P43311 (Sultana berry cDNA) (*1*), PPO_MALDO P43309 (apple) (*37*), PPO_VICFA Q06215 (bean) (*6*), PPO2_IPOBA Q9MB14, Q84 V52, Q9ARD3 (sweet potato), PPOB_SOLTU Q06355 (potato) (*4*), PPOD_SOLLC Q08306 (tomato) (*3*), PPO_SPIOL P43310 (spinach) (*38*), PPOA_SOLLC Q08303 (tomato) (*3*). Identical residues and conservative substitutions are shown in bold. * indicates grenache leaf cDNA P93622. ** indicates sultana berry cDNA P43311. Residues that are different between the two grape PPOs are highlighted. Alignments of the common central domain of tyrosinase (accession number PF00264) can be viewed at http://www.sanger.ac.uk/Software/Pfam/data/jtml/seed/PF00264.shtml.

span of the PPO C-terminus would be phosphorylated. The occurrence of six potential myristoylation sites (**Figure 1**) also suggests association with a membrane (*34*). We identified potential N-glycosylation sites at residues 19 and 40; in animal tyrosinases, 5 to 6 such sites have been identified (*35*, *36*).

Aligned sequences of plant PPOs are shown in **Figure 2**. These include the two grape sequences, P93622_VITVI (this work) and PPO_VITVI (*1*), apple, bean (*6*), sweet potato, potato (*4*), two tomato sequences (*3*), and spinach (*38*). The two grape cDNAs share 99% identity. Our Southern analysis is in accordance with that of Dry and Robinson (*1*) and suggests the existence of a single gene for Grenache grape PPO (data not shown). In general, the amino acid differences between the two grape cDNAs occur in regions without conserved secondary structure motifs; the substitutions F for S at position 11 and K for N at position 444 also occur in other plant PPOs. The P at position 243 is conserved, and most family members have F and not I in the position equivalent to 240, although hemocyanin has V and not F (see NCBI pfam00264.12 at http://www.ncbi.nlm.nih.gov/Structure). We note that the electron density (see below) suggested F rather than I at position 240 and P rather than A at position 243, which are consistent with the sequence of sultana PPO (*1*), but V rather than A at position 340, which is consistent with our sequencing results.

Purification of PPO from Grape Berries. Grape berry extract was chromatographed on Sephadex G-75 (**Figure 3A**). The fractions comprising peak 2 were pooled and subjected to anion exchange chromatography (**Figure 3B**), producing two activity peaks, with a major peak eluting at about 0.1 M NaCl and a smaller peak eluting during the steeply ramped salt wash. The fractions corresponding to peak 1 (**Figure 3B**) were again subjected to size exclusion chromatography, but using a Superose-R 12 column. This step yielded one major peak with three shoulders (**Figure 3C**). The four peaks containing activity were submitted to SDS-PAGE, and the gels were stained for protein (*31*) and

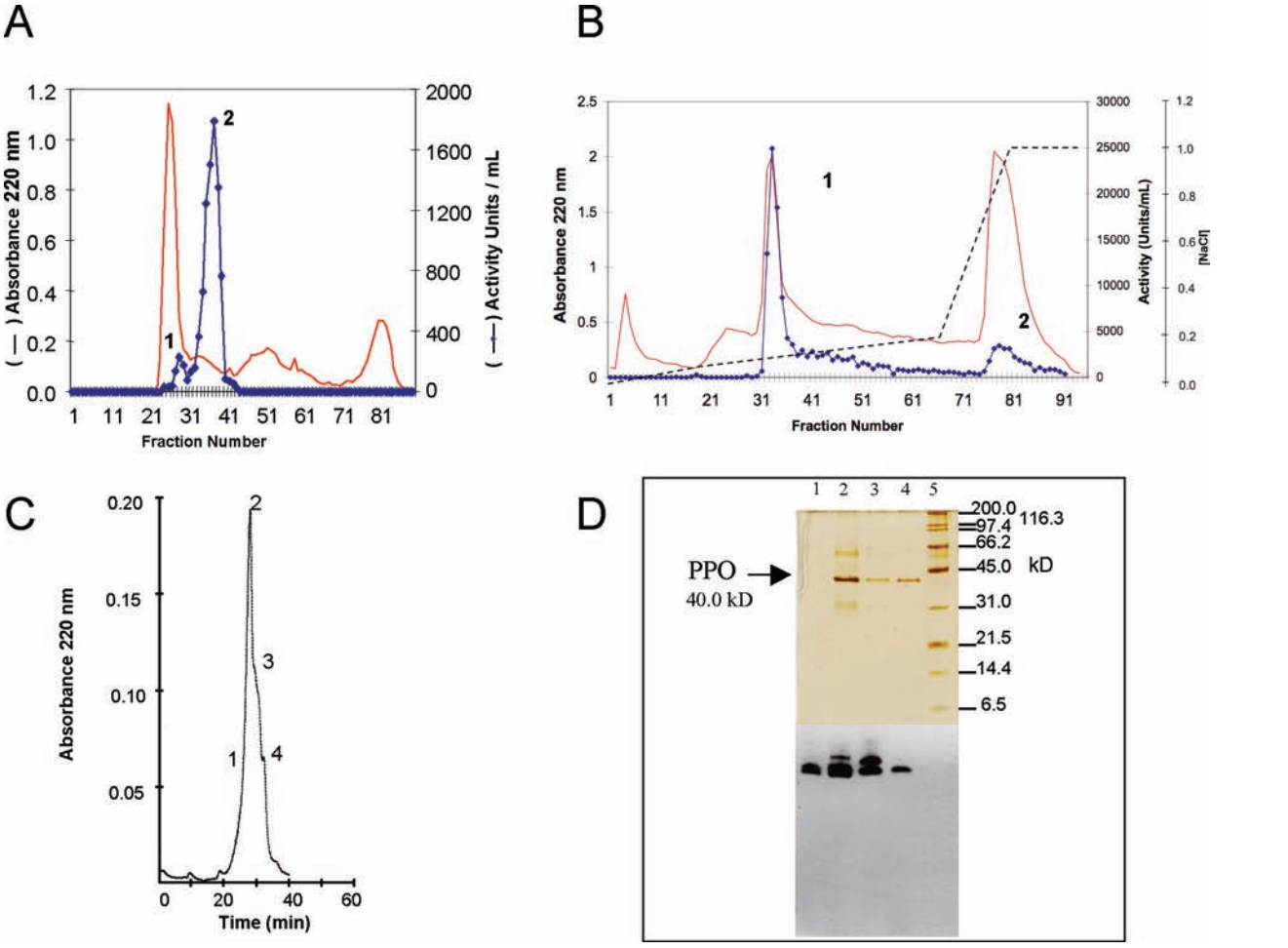

Figure 3. Purification of grenache berry PPO. (**A**) Gel filtration chromatography of combined ammonium sulfate pellets after dialysis was applied to a Sephadex G-75 (167 × 1.7 cm^2) column, equilibrated with 5 mM sodium phosphate, pH 8.0, and eluted with the same buffer at a flow rate of 0.3 mL/min; 4.0 mL fractions were collected. The fractions containing peak 2 were combined for ion exchange chromatography. (**B**) Anion-exchange chromatography using an Econo-Pac High Q cartridge (1 × 5 cm^2). Elution was obtained using a NaCl gradient from 0 to 0.2 M NaCl in 5 mM sodium phosphate, pH 8.0, for 136 min at a flow rate of 1.0 mL/min, collecting 2.0 mL fractions. After 166 min, the gradient was increased to 1.0 M NaCl, eluting a second, smaller peak with PPO activity. (**C**) HPLC chromatography of the fractions corresponding to peak 1 of part **B** on a Superose 12 HR10/30 column, equilibrated with 10 mM Tris-HCl, pH 7.5. (**D**) SDS-PAGE. Lanes 1−4 contained fractions 1−4 from the HPLC experiment shown in part **C**; lane 5, molecular mass markers. Upper gel: silver stain, fully denatured protein; lower gel: activity stain using 25 mM 4-*tert*-butylcatechol and 25 mM 4-amino-*N*,*N*-diethylaniline sulfate. Incompletely denatured protein was used for the activity gel, and bands might not represent different molecular weights.

activity. Peak number 4, which had an apparent mass of 40 kDa, showed a single protein and a single activity band and was used for crystallization and X-ray analysis.

Basic Symmetry Characterization of the Crystal Structure of Grenache Berry PPO. The crystals obtained (**Figure 4**) belonged to the orthorhombic space group $C222_1$ with cell dimensions $a = 60.03$, $b = 120.77$, and $c = 140.80$ Å, and $\alpha = \beta = \gamma = 90°$. **Table 2** shows the characteristics of the crystals of three different PPOs. The basic symmetry of these three crystals is completely different in terms of cell parameters and crystal packing, which suggests the possibility of additional variability within the plant enzymes, as has been observed for animal tyrosinases at the whole enzyme level (*39*).

Three-Dimensional Structure of Grenache Berry PPO. All data and statistics obtained after processing the X-ray diffraction are shown in **Table 3**. These data yielded a unique data set of 183,718 reflections with an R_{merge} of 0.125%. One hundred twenty-eight water molecules were in the structure, and the crystals contained 46.0% solvent, as determined by the formula of Matthews (*40*). The program PROCHECK (*41*) indicated that almost all residues (96.74%) in the asymmetric unit were located in the most favorable regions of the Ramachandran plot, with 2.08% of the residues in the allowed region and 1.14% (4 residues) in the disallowed region.

The overall structure of the polyphenol oxidase from *V. vinifera* is a monomeric protein of 38.4 kDa. It is an ellipsoid with dimensions 56.7 × 48.0 × 48.3 $Å^3$ (**Figure 5**). The secondary structure is primarily α-helical with the core of the protein formed by a four-helix-bundle composed of α-helices α4, α5, α12, and α14 (**Figure 5A**). **Figure 5B** shows overlapping images of the three existing PPO structures. There are a few areas where the folding is slightly different. For the most part, these differences occur on the surface and do not involve changes in α-helices or β-strands.

N-Terminal Processing. PPO is a nuclear-encoded protein that is nonetheless associated with chloroplasts. Using *in vitro*-translated tomato gene product and pea plastids, Sommer and co-workers (*9*) found that the initial translated product was indeed 67 kDa in size. This precursor was processed to a 62 kDa product in the chloroplast stroma and further processed to 59 kDa in the thylakoid lumen. Their interpretation of these events was consistent with the primary structure of the translated product, which exhibited a 48-residue hydroxyamino acid-rich N-terminal sequence, associated with targeting to the stroma. Processing was

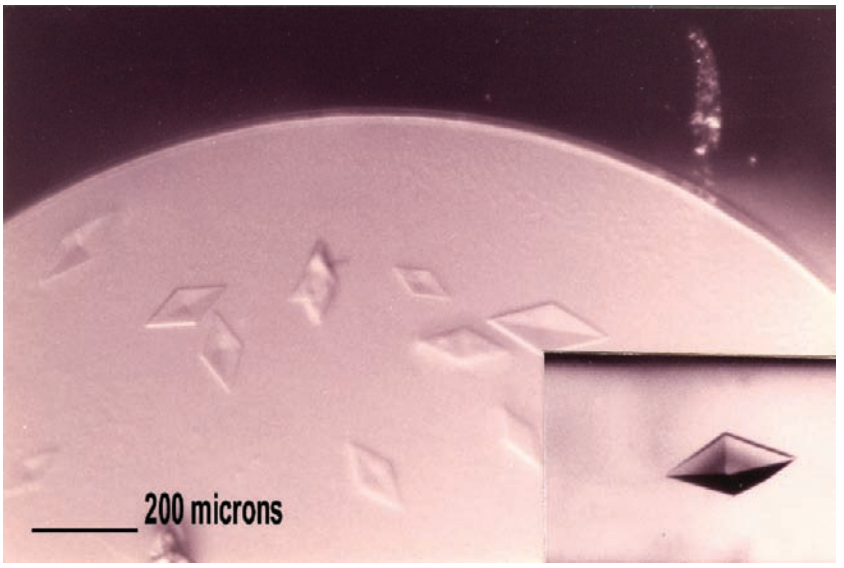

Figure 4. Crystals of PPO obtained by the hanging-drop vapor-diffusion method. The inset shows the largest crystal, 200 μm in the longest dimension, which was used to obtain a full data set.

Table 2. X-ray Characterization of the Basic Symmetry for Crystals of Different PPOs

PPO (space group)	cell parameters (Å), angles (deg)	monomers in the asymmetric unit
grenache berry ($C222_1$)	a = 60.03, b = 120.77, c = 140.80	one
sweet potato ($P2_12_12$)	a = 46.00, b = 157.60, c = 55.80	four
sweet potato ($P2_1$)	a = 45.70, b = 165.80, c = 51.60, β = 97.10	two

presumed to occur between Lys and Val residues in the sequence KVSC, which is conserved among the PPOs shown in **Figure 2**. The lumen-targeting domain is defined by a pair of Arg residues, immediately followed by NVLLGL and a hydrophobic run of about 20 residues, predicted to be myristoylated and therefore membrane bound. The C-terminal end of that targeting peptide was assigned to a Thr residue homologous to A104 of P93622_VITVI (**Figure 1**), immediately before a conserved proline. This Ala residue appears in our X-ray structure as the N-terminus of the mature protein. Based on these two processing events, which are typical of transit peptides for nuclear-encoded, plastid-targeted proteins, the product should have a molecular weight of 56.7 kDa. Sommer and co-workers (*9*) suggested that this second N-terminal processing step occurs on the stromal face of the thylakoid membrane and is catalyzed by a membrane-bound protein. Indeed, this run of ca. 20 hydrophobic amino acids between the pair of Arg residues and the site of cleavage suggests that the transit peptide is a membrane-spanning region. A significant amount of the N-terminally processed protein (59 kD in the tomato enzyme) was found soluble in the thylakoid lumen of pea chloroplasts in their *in vitro* study, indicating that it is released from the putative transmembrane domain. There was an indication that the extent of the second proteolytic cleavage depends on the developmental stage of the plastids. These results are also consistent with the N-terminal sequence and processing of lumen-located spinach PPO (*33*, *42*).

C-Terminal Processing. These N-terminal processing steps would yield a 56.7 kD protein and therefore do not explain the observed molecular weight of the crystallized *V. vinifera* PPO.

Table 3. Crystallographic Statistics[a]

Data Collection	
space group	$C222_1$
unit cell parameters (Å)	a = 60.03, b = 120.77, and c = 140.80
resolution, Å (highest shell)	37.06−2.20 (2.26−2.20)
number of molecules in the asymmetric unit	1
total/unique reflections	183718/23748
redundancy	6.96 (5.41)
$I/\sigma I$	8.1 (2.9)
completeness, %	99.8 (97.8)
R_{merge}	0.125 (0.487)
Refinement	
R (working) (%)	20.1
R-free (%)	25.2
rms deviation of ideality	
bond length (Å)	0.22
bond angles (deg)	1.95
no. of atoms per asymmetric unit	2847
Average B-Factors (Å^2)	
overall	44.82
protein	37.65
water	43.68%
copper	53.15

[a] Data cutoff for refinement was (Fourier coefficient amplitudes, F) $F > 0$. The values in parentheses are for the outer resolution shell. $I/\sigma I$ is the ratio of the mean intensity to the mean standard deviation of the intensity.

Further processing of PPOs in the hemolymph of arthropods is accomplished by a serine protease that is activated by bacterial cell wall components (*10*). This processing in plants and fungi was discussed by van Gelder and co-workers (*8*) and more recently by Marusek and co-workers (*43*); the latter discussion included comparisons to related proteins, the hemocyanins. The products encoded by genes from plants and higher eukaryotes show reasonable homology and can be divided into three domains: an N-terminal domain containing signal and transit peptides, a central domain containing binding sites for two copper centers, and a C-terminal domain of unknown significance. The products of fungal and bacterial genes lack the N-terminal domain, since these organisms also lack the plastids to which the plant PPO is

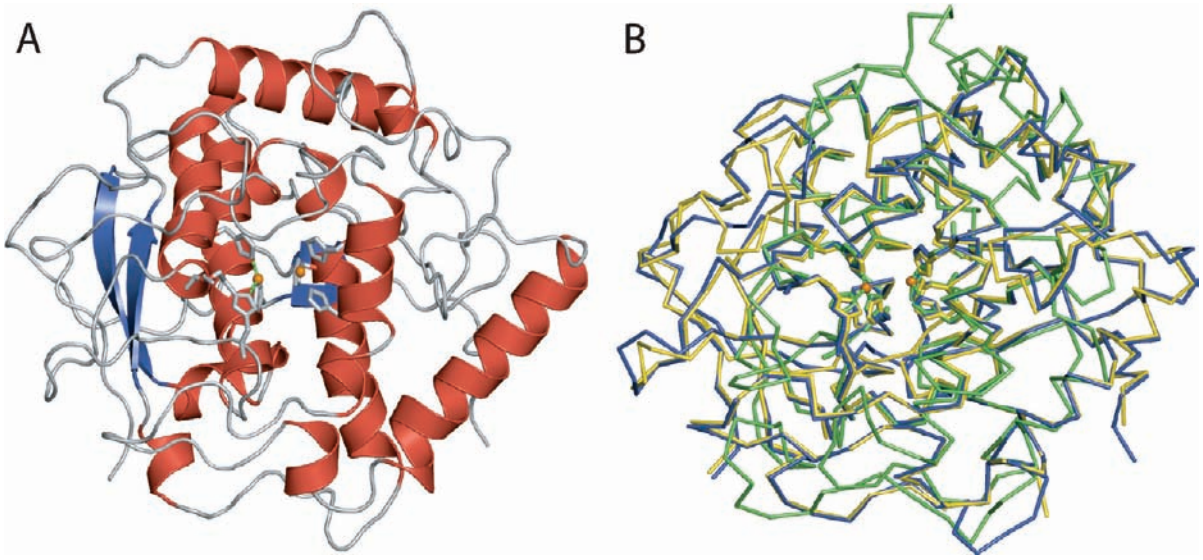

Figure 5. X-ray structure of PPO from *V. vinifera*. (**A**) Ribbon model showing the overall ellipsoidal shape, two β-sheets, and the dicopper center within a four-helix bundle. (**B**) Cα representation of *V. vinifera* PPO (blue) overlapping with those of PPO from sweet potato (yellow) (*18*) and *Neurospora crassa* (green) (PDB code 1wx2). The superposition of the *V. vinifera* protein structure with that of sweet potato showed a 0.76 Å root-mean-square (rms) deviation for 325 Cα pairs, and that for the monomer of the *N. crassa* enzyme showed a 1.11 Å deviation for 170 Cα pairs; the *V. vinifera* PPO structure was the reference structure in both cases.

targeted, and the targeting sequence of the mammalian product is thought to direct it to melanosomes in melanocytes (*44*). All of the PPOs that have been studied are known to undergo significant processing to cleave the C-terminal domain, and gene sequences suggest the existence of similar processing sites in a host of related proteins. Marusek and co-workers (*43*) have identified a "linker sequence", which begins shortly after an invariant "tyrosine motif" (YQY beginning at position 328 in the *V. vinifera* protein, residue 431 predicted in P93622_VITVI) that connects the central domain with the C-terminal domain. They postulate that C-terminal processing occurs within the linker region, which they predict is unstructured and therefore available to protease attack. Our electron density map shows P339 (P236 in the crystal structure) as the C-terminal residue, which occurs only seven residues into the linker region, a region in which secondary structure prediction algorithms do not assign structure in the *V. vinifera* protein. This Pro residue is on the surface of the protein and could easily be the site of proteolysis by peptidyl-Lys metalloendopeptidase-like activity. However, because of the position of the proline on the surface, it is also possible that there are additional C-terminal amino acids that are either mobile or disordered in the crystal and do not produce a distinct electron density map. The sequence in that region is WLPKNTKAKAK, in which only the Trp is conserved among plant PPO sequences, but numerous Lys residues occur nearby, though not in precisely homologous positions, to the lysine that follows the supposed C-terminal proline. Tryptic activity would leave a C-terminal PK sequence, and it is possible that a C-terminal, surface lysine might not be sufficiently rigidly structured to yield an interpretable electron density map.

Despite the evidence from bioinformatics, the fact that the proteolytic processing steps occur in grape berry PPO is somewhat surprising, in light of the fact that both N-terminal cleavages are associated with targeting to a specific compartment within the chloroplast, and the C-terminal cleavage is thought to be carried out by enzymes in the thylakoid lumen. However, this protein was isolated from the berry, which contains relatively few chloroplasts, localized near the skin surrounding a large mesocarp. The fact that the grape berry PPO has the N- and C-termini predicted from processing arguments suggests (1) that the berry PPO arises from a related gene that encodes a smaller protein, (2) that the message is transcribed from the 1824-bp orf but processed before translation, (3) that the majority of PPO in the berry is processed in the thylakoid lumen and then either secreted into the cytoplasm or released during extraction, or (4) that processing occurs in the cytoplasm by cytoplasmic enzymes. To investigate the first possibility, we searched the complete genome of Pinot Noir (*45*) and found four homologues, all in chromosome 10 contigs. However, it is not clear if more than one of them is expressed, since the Genebank grape transcriptome information does not seem to be complete. Our Southern analysis indicates the expression of only one gene in Grenache grapes. Although we cannot rule out the third possibility, the fourth explanation also seems plausible. We suggest that the nuclear-encoded protein is targeted to the plastids in cells that contain plastids and to the cytoplasm of mesocarp cells, where proteolytically sensitive bonds are cleaved by cytoplasmic proteases. Alternatively, N-terminal processing could occur in the plastid, followed by secretion and C-terminal processing in the cytoplasm.

A recent proteomic study of ripe grape (*cv.* Gamay noir) berries (*46*) detected three major proteins corresponding to the deduced PPO sequence, one of about 36 kDa and two of about 20 kDa, but with slightly different p*I* values. The most C-terminal tryptic peptide found in the 36 kDa protein corresponded to YQYQDIPIPWLPK (*47*), which is one residue beyond the C-terminal residue that we were able to observe in the electron density map. This result is entirely consistent with our observations. On the other hand, although the majority of peptides found in the 20 kDa spots are C-terminal to the end of the 36 kDa protein, there is one surprising exception: both C-terminal peptides contained the tryptic peptide MWNIWKTIGGK, which begins inside the 36 kDa protein, about 50 residues from its C-terminus. This observation suggests that if the C-terminal proteolytic processing does occur in the berry, such processing might be less specific than processing in the thylakoid, leading to multiple active isoforms. This suggestion is supported by the data shown in **Figure 3**. The size exclusion column yielded a major peak with three shoulders. Although the size exclusion separation

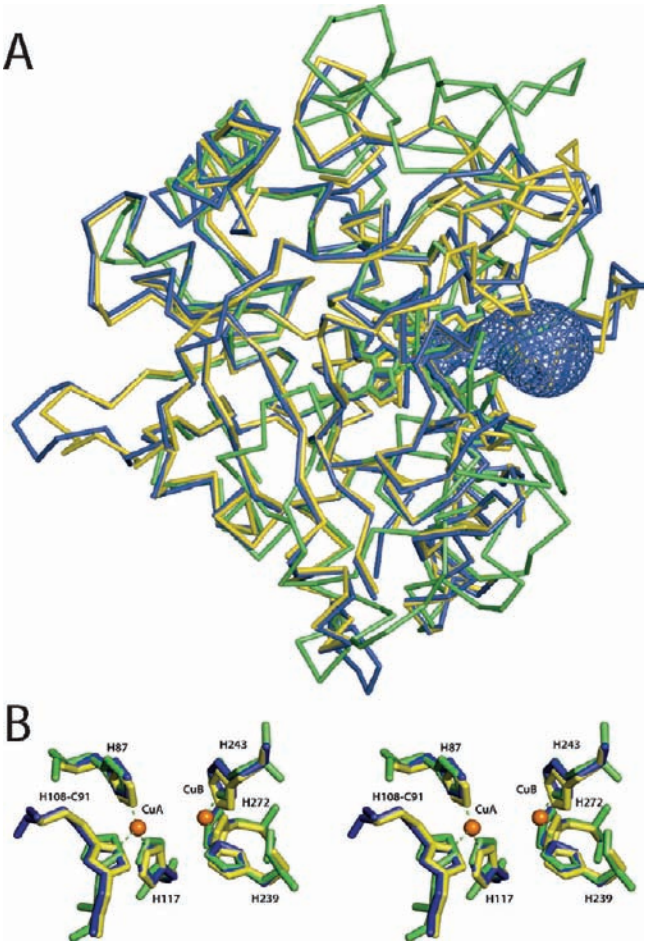

Figure 6. Active site of PPO, showing *V. vinifera* PPO (blue) and sweet potato (yellow) and *N. crassa* enzyme (green) (PDB 1wx2). (**A**) Access of the dicopper center to the surface of the enzyme as determined using CAVER (*49*). This structure is rotated by 90° from those in **Figure 5** for clarity. (**B**) Detail of the coordination of the copper ions by active-site His side chains and of the thioether linkage between C91 and H108 (*V. vinifera* PPO numbering). The internuclear distances were as follows: Cu−Cu, 4.17 Å; CuA to H87, 2.07 Å; H108, 2.16 Å; H117, 2.35 Å; CuB to H239, 2.04 Å; H243, 2.15 Å; H272, 2.02 Å.

indicated slightly different hydrodynamic sizes, the SDS gel demonstrated that the sizes of the major proteins were very similar. It is therefore likely that C-terminal processing occurred at more than one site, although alternative splicing of the message is also possible. This explanation is consistent both with the proteomic study, which is designed to detect distinguishable isoforms, and with our crystallographic study, which focused only on the homogeneous fraction selected for crystallization. There is a second surprising conclusion from the proteomic study, which demonstrated that the C-terminal fragments (i.e., the 20 kDa peptides) persist in the tissue at levels comparable to that of the active enzyme. Whether or not they have a function is not known.

PPO activity and proteolytic processing have recently been studied in olive tree (*Olea europaea* cv. "Picual") leaves and fruit (*48*). Although the leaf PPO had a molecular weight of 50 kDa, the fruit enzyme had a molecular weight of 55 kDa and appeared to be a dimer of 27.7 kDa subunits. During the last stages of maturation, a second protein with PPO activity with an apparent molecular weight of 36 kDa appeared in the fruit but not in the leaves. The leaf enzyme presumably functions in wound response, but the fruit enzyme is involved in the formation of numerous phenolic compounds that are produced during ripening. It is therefore not surprising that PPO in the chloroplast-rich grape leaves might be processed differently from that in chloroplast-poor grape berries.

Despite the existence of predicted glycosylation and phosphorylation sites (**Figure 1**), we observed no electron density corresponding to covalent modification of any side chains. Many of the predicted sites occur outside the mature protein sequence, and we have no evidence concerning their modification or the significance of such modification. The mature, active form of the enzyme that we crystallized is also devoid of phosphorylation and glycosylation. It is also likely that our purification and the crystallization process selected against modified forms. Phosphorylated isoforms, in particular, would have been removed by the anion exchange separation (e.g., peak 2 in **Figure 3B**). In any case, none of these modifications is required for activity.

Active Site. As in *N. crassa* PPO and lobster hemocyanin, three His residues bind each of the two copper ions. The 3D structure of the α subunit of domain 2 of *Panulirus interruptus* hemocyanin contains six His residues coordinating the two Cu ions as well. These His residues are located on four α-helices that fold in proximity to each other (4 helix bundle motif) (*20*). By similarity to *N. crassa* PPO, H211, H220, H342, H346, and H375 of their deduced sequence were designated as Cu binding residues in ppo_vitvi (*1*). Tryptophan occurs in conserved positions close to the proposed active site histidines. The sequence homologies shown in **Figure 2** indicate some residues that are absolutely conserved among the plant PPOs.

The X-ray data indicate that the active site is located in the central part of this group of helices, surrounded by α-helices 3 and 9 and short β-strands. The application CAVER (*49*) shows a clear path from the surface of the protein to the active-site copper ions in all three of the known PPO structures (**Figure 6A**). From the X-ray data, it can be seen that nine conserved His, six conserved

Scheme 2

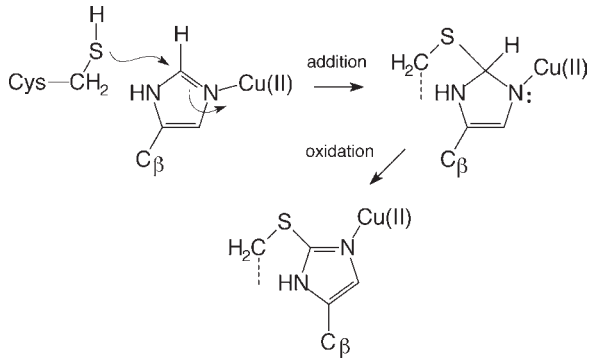

Trp, seven of the eight conserved Phe, three of the seven conserved Arg, and seven of the twelve conserved Leu residues are in the active site region. Each of the two active site copper ions is coordinated by three histidine side chains contributed by the helices of the α-bundle. As shown in **Figure 6B**, one copper ion (CuA) is coordinated by H87, H108, and H117 (residues 190, 211, and 220 in the deduced sequence). H87 is located in the central part of the helix α-4; H108 precedes helix α-5, and finally H117 is located at the beginning of helix α-5. The second catalytic copper ion (CuB) is coordinated by H239, H243, and H272 (342, 346, and 375 in the deduced sequence), which are located at the beginning and at the end of helices α-12 and α-14, respectively. The structure is stabilized along the N-terminus by two disulfide bridges located between C11 and C26 and between C25 and C88 (corresponding to residues 114, 129, 128, and 191, respectively, in the deduced structure). Of the three remaining Cys residues in the sequence, C52 is lost by N-terminal processing, C91 (C194 in the deduced sequence) is engaged in a novel thioether bond to the ring of H108, and C320 (423 in the deduced sequence) exists as a free sulfhydryl group and is not conserved throughout the sequences shown in **Figure 2**.

It appears that the majority of plant PPOs that have been examined exist in a mature form that is latent (*8*). The latent form is quite stable (*50*), at least in the carrot enzyme, whereas, once activated, (e.g., refs *13* and *51*), it undergoes self-inactivation. These observations are consistent with the function of PPO as a wound-response enzyme. The mechanism of activation remains obscure. In this regard, it is significant that H108, which is part of the coordination ring with CuA, is covalently bound to C91 (**Figure 6B**), as was discovered by Lerch during peptide sequencing (*19*). The cysteine sulfur atom and histidine ring are coplanar in the X-ray structure, indicating that the ring exists as imidazole, as opposed to dihydroimidazole. Klabunde suggested that the bond might be formed via a free radical reaction, in analogy to a Cys-Tyr cross-link proposed for galactose oxidase. But imidazole is not aromatic, and a simple addition reaction could occur, followed by oxidation to restore the planar geometry. The initial adduct would be a substituted dihydroimidazole (**Scheme 2**), the formation of which is aided by the presence of the copper ion. The imidazole C4 and the ligand nitrogen would be tetrahedral in this structure; the tautomers of the initial and final structures proposed in the scheme are suggested by X-ray structures of Cu(II)-imidazole complexes (*52*). We suggest that this is the latent form of PPO or one of the latent forms. We further suggest that when oxygen binds to the copper ions at the active site, the dihydroimidazole is oxidized to imidazole, which causes a local conformation change that alters the coordination geometry to that observed in the X-ray structures. This cross-link is not responsible for the observed turnover-based inactivation of the enzyme (*17*), because such inactivation requires exposure to the phenolic substrate as well as O_2 (*13*, *17*, *51*) and because the crystals are composed of active protein. It is tempting, however, to suggest that the oxidation of the resulting adduct constitutes the final activation step for PPO. C91 is the only cysteine conserved in the mature protein across plant and fungal species (*43*). A cysteine residue homologous to C91 is absent in octopus hemocyanin (homologies according to ref *43*), but another cysteine, residue 2560, is attached via a thioether bridge to H2562 (*53*), which is homologous to H108 of the *V. vinifera* PPO. These observations suggest that the thioether bridge to the ligand imidazole ring is essential. An inactive C91-substituted mutant would not be a definitive test of this suggestion, and the concept of activation for hemocyanins is equally difficult to test.

As pointed out by van Gelder and others (*8*), many treatments or conditions are capable of activating latent PPO, including treatment with anionic detergents; proteolytic cleavage is often proposed as the activation step. Robinson and Dry (*54*) isolated a 60 kD protein from *V. faba* leaves and found that it was hydrolyzed to a 45 kD "mature form"; however, the relevance to activation is obscured by the fact that both forms of the protein were activated by the inclusion of 2 mM SDS and were equally active. Their data showed that this C-terminal processing step neither prevented nor caused full activation of the enzyme (in SDS), although such cleavage could constitute a portion of the activation step, *in vivo*.

Tyrosinase Activity. Our assays of monophenol oxygenase activity in the protein used for the crystallization indicate that grape berry PPO does not catalyze this reaction. This result is consistent with the similarity between the active sites of the grape enzyme and the sweet potato enzyme (*18*), which also possesses catecholase but not tyrosinase (monophenol oxygenase) activity. The residue E236, proposed to function as a general acid/base in diphenol oxidation (*18*), is conserved in the *V. vinifera* enzyme. Without a structure of an enzyme with monophenol oxygenase activity, we cannot determine what might be lacking in the grape enzyme that prevents it from catalyzing the oxygenation reaction.

ABBREVIATIONS USED

PPO, polyphenol oxidase; L-DOPA, L-dihydroxyphenylalanine; EDTA, ethylaminediamine tetraacetic acid; CTAB, cetyl trimethylammonium bromide; PCR, polymerase chain reaction; RACE-PCR, rapid amplification of cDNA ends; PVPP, polyvinyl polypyrrolidone.

ACKNOWLEDGMENT

The authors thank J-E Sarry and C. Romieu for helpful discussions and for sharing unpublished data with us, and V. Llaca for helpful discussions.

Supporting Information Available: Supplemental Table 1 showing the complete sequence of cDNA derived from leaf RNA of a white variety of Grenache grapes (*V. vinifera* L. cv. Grenache) and its deduced amino acid sequence. Supplemental Figure 1 showing the active site of Grenache PPO with electron density contours. This material is available free of charge via the Internet at http://pubs.acs.org.

LITERATURE CITED

(1) Dry, I. B.; Robinson, S. P. Molecular cloning and characterisation of grape berry polyphenol oxidase. *Plant Mol. Biol.* **1994**, *26* (1), 495–502.

(2) Martinez, M. V.; Whitaker, J. R. The biochemistry and control of enzymatic browning. *Trends Food Sci. Technol.* **1995**, *6*, 195–200.

(3) Newman, S. M.; Eannetta, N. T.; Yu, H.; Prince, J. P.; de Vicente, M. C.; Tanksley, S. D.; Steffens, J. C. Organisation of the tomato polyphenol oxidase gene family. *Plant Mol. Biol.* **1993**, *21* (6), 1035–1051.
(4) Hunt, M. D.; Eannetta, N. T.; Yu, H.; Newman, S. M.; Steffens, J. C. cDNA cloning and expression of potato polyphenol oxidase. *Plant Mol. Biol.* **1993**, *21* (1), 59–68.
(5) Thygesen, P. W.; Dry, I. B.; Robinson, S. P. Polyphenol oxidase in potato. A multigene family that exhibits differential expression patterns. *Plant Physiol.* **1995**, *109* (2), 525–31.
(6) Cary, J. W.; Lax, A. R.; Flurkey, W. H. Cloning and characterization of cDNAs coding for *Vicia faba* polyphenol oxidase. *Plant Mol. Biol.* **1992**, *20* (2), 245–53.
(7) Jolley, R. L.; Nelson, R. M.; Robb, D. A. The multiple forms of mushroom tyrosinase. *J. Biol. Chem.* **1969**, *244* (12), 3251–3257.
(8) van Gelder, C.; Flurkey, W.; Wichers, H. Sequence and structural features of plant and fungal tyrosinases. *Phytochemistry* **1997**, *45* (7), 1309–1323.
(9) Sommer, A.; Ne'eman, E.; Steffens, J. C.; Mayer, A. M.; Harel, E. Import, targeting, and processing of a plant polyphenol oxidase. *Plant Physiol.* **1994**, *105* (4), 1301–11.
(10) Aspán, A.; Sturtevant, J.; Smith, V.; Söderhäll, K. Purification and characterization of a prophenoloxidase activating enzyme from crayfish blood cells. *Insect Biochem.* **1990**, *20* (7), 709–718.
(11) Thipyapong, P.; Mahanil, S.; Bhonwong, A.; Attajarusit, J.; Stout, M. J.; Steffens, J. C. Increasing resistance of tomato to lepidopteran insects by overexpression of polyphenol oxidase. *Acta Hortic.* **2004**, *724*, 29–38.
(12) Mayer, A. Polyphenol oxidases in plants and fungi: Going places? A review. *Phytochemistry* **2006**, *67*, 2318–2331.
(13) Golan-Goldhirsh, A.; Whitaker, J. R. Kcat inactivation of mushroom polyphenol oxidase. *J. Mol. Catal.* **1985**, *32*, 141–147.
(14) Rathgen, A.; Robinson, S. Aberrant processing of polyphenol oxidase in a varegated grapevine mutant. *Plant Physiol.* **1992**, *99*, 1619–1625.
(15) Lerch, K. Neurospora tyrosinase: structural, spectroscopic and catalytic properties. *Mol. Cell. Biochem.* **1983**, *52* (2), 125–38.
(16) Lerch, K. Tyrosinase: Molecular and active-site structure. In *Enzymatic Browning and Its Prevention*; Lee, C. Y., Whitaker, J. R., Eds.; ACS Publications: Washington, DC, 1995; Vol. 600, pp 64−80.
(17) Whitaker, J. R. Polyphenol oxidase. In *Food Enzymes: Structure and Mechanism*; Wong, D. W. S., Ed.; Chapman and Hall: New York, 1995; pp 284−320.
(18) Klabunde, T.; Eicken, C.; Sacchettini, J. C.; Krebs, B. Crystal structure of a plant catechol oxidase containing a dicopper center. *Nat. Struct. Biol.* **1998**, *5* (12), 1084–90.
(19) Lerch, K. Primary structure of tyrosinase from *Neurospora crassa*: II Complete amino acid sequence and chemical structure of a tripeptide containing an unusual thioether. *J. Biol. Chem.* **1982**, *257*, (10), 6414−6419.
(20) Volbeda, A.; Hol, W. G. Crystal structure of hexameric haemocyanin from *Panulirus interruptus* refined at 3.2 Å resolution. *J. Mol. Biol.* **1989**, *209* (2), 249–79.
(21) Franke, K. E.; Liu, Y.; Adams, D. O. Yield and quality of RNA from grape berries at different developmental stages. *Am. J. Enol. Vitic.* **1995**, *46* (3), 315–318.
(22) Bowers, J. E.; Bandman, E. B.; Meredith, C. P. DNA Fingerprint Characterization of Some Wine Grape Cultivars. *Am. J. Enol. Vitic.* **1993**, *44* (3), 266–274.
(23) Frohman, M. A.; Dush, M. K.; Martin, G. R. Rapid production of full-length cDNAs from rare transcripts: amplification using a single gene-specific oligonucleotide primer. *Proc. Natl. Acad. Sci. U.S.A.* **1988**, *85* (23), 8998–9002.
(24) Innis, M. A.; Gelfand, D. H. Optimization of PCRs. In *PCR Protocols, a Guide to Methods and Applications*; Innis, M. A., Gelfand, D. H., Sninsky, J. J., White, T. J., Eds.; Academic Press, Inc.: San Diego, 1990; pp 3−12.
(25) Saiki, R. K.; Gelfand, D. H.; Stoffel, S.; Scharf, S. J.; Higuchi, R.; Horn, G. T.; Mullis, K. B.; Erlich, H. A. Primer-directed enzymatic amplification of DNA with a thermostable DNA polymerase. *Science* **1988**, *239* (4839), 487–91.
(26) Altschul, S. F.; Gish, W.; Miller, W.; Myers, E. W.; Lipman, D. J. Basic local alignment search tool. *J. Mol. Biol.* **1990**, *215* (3), 403–10.
(27) Bradford, M. M. A rapid and sensitive method for the quantitation of microgram quantities of protein utilizing the principle of protein-dye binding. *Anal. Biochem.* **1976**, *72*, 248–54.
(28) Joslyn, M. A.; Ponting, A. Enzyme-catalyzed oxidative browning of fruit products. *Adv. Food Res.* **1950**, *3*, 1–44.
(29) Rescigno, A.; Sollai, F.; Rinaldi, A. C.; Soddu, G.; Sanjust, E. Polyphenol oxidase activity staining in polyacrylamide electrophoresis gels. *J. Biochem. Biophys. Methods* **1997**, *34* (2), 155–9.
(30) Duckworth, H.; Coleman, J. Physicochemical and kinetic properties of mushroom tyrosinase. *J. Biol. Chem.* **1970**, *245* (7), 1613–1625.
(31) Blum, H.; Beier, H.; Gross, H. J. Improved silver staining of plant proteins, RNA and DNA in polyacrylamide gels. *Electrophoresis* **1987**, *8* (2), 93–99.
(32) Collaborative Computational Project, N., The CCP4 Suite: Programs for Protein Crystallography. *Acta Crystallogr.* **1994**, *D50*, 760−763.
(33) Sokolenko, A.; Fulgosi, H.; Gal, A.; Altschmied, L.; Ohad, I.; Herrmann, R. G. The 64 kDa polypeptide of spinach may not be the LHCII kinase, but a lumen-located polyphenol oxidase. *FEBS Lett.* **1995**, *371* (2), 176–80.
(34) Martin, M.; Busconi, L. Membrane localization of a rice calcium-dependent protein kinase (CDPK) is mediated by myristoylation and palmitoylation. *Plant J.* **2000**, *24*, 429–435.
(35) Inagaki, H.; Bessho, Y.; Koga, A.; Hori, H. Expression of the tyrosinase-encoding gene in a colorless melanophore mutant of the medaka fish, *Oryzias latipes*. *Gene* **1994**, *150* (2), 319–324.
(36) Muller, G.; Ruppert, S.; Schmid, E.; Schutz, G. Functional analysis of alternatively spliced tyrosinase gene transcripts. *EMBO J.* **1988**, *7* (9), 2723–2730.
(37) Boss, P. K.; Gardner, R. C.; Janssen, B. J.; Ross, G. S. An apple polyphenol oxidase cDNA is up-regulated in wounded tissues. *Plant Mol. Biol.* **1995**, *27* (2), 429–33.
(38) Hind, G.; Marshak, D. R.; Coughlan, S. J. Spinach thylakoid polyphenol oxidase: cloning, characterization, and relation to a putative protein kinase. *Biochemistry* **1995**, *34* (25), 8157–64.
(39) Jaenicke, E.; Decker, H. Tyrosinases from crustaceans form hexamers. *Biochem. J.* **2003**, *371*, 515–523.
(40) Matthews, B. X-ray crystallographic studies of proteins. *Annu. Rev. Phys. Chem.* **1976**, *27*, 493–523.
(41) Laskowski, R.; MacArthur, M.; Moss, D.; Thornton, J. PROCHECK: a program to check the stereochemical quality of protein structures. *J. Appl. Crystallogr.* **1993**, *26* (2), 283–291.
(42) Gal, A.; Herrmann, R.; Lottspeich, F.; Ohad, I. Phosphorylation of cytochrome b6 by the LHC II kinase associated with the cytochrome complex. *FEBS Lett.* **1992**, *298* (1), 33–35.
(43) Marusek, C.; Trobaugh, N.; Flurkey, W.; Inlow, J. Comparative analysis of polyphenol oxidase from plant and fungal species. *J. Inorg. Biochem.* **2006**, *100*, 108–123.
(44) Yamaguchi, T.; Brenner, M.; Hearing, V. J. The regulation of skin pigmentation. *J. Biol. Chem.* **2007**, *282* (38), 27557–27561.
(45) Velasco, R.; Zharkikh, A.; Troggio, M.; Cartwright, D. A.; Cestaro, A.; Pruss, D.; Pindo, M.; FitzGerald, L. M.; Vezzulli, S.; Reid, J.; Malacarne, G.; Iliev, D.; Coppola, G.; Wardell, B.; Micheletti, D.; Macalma, T.; Facci, M.; Mitchell, J. T.; Perazzolli, M.; Eldredge, G.; Gatto, P.; Oyzerski, R.; Moretto, M.; Gutin, N.; Stefanini, M.; Chen, Y.; Segala, C.; Davenport, C.; Dematt, L.; Mraz, A.; Battilana, J.; Stormo, K.; Costa, F.; Tao, Q.; Si-Ammour, A.; Harkins, T.; Lackey, A.; Perbost, C.; Taillon, B.; Stella, A.; Solovyev, V.; Fawcett, J. A.; Sterck, L.; Vandepoele, K.; Grando, S. M.; Toppo, S.; Moser, C.; Lanchbury, J.; Bogden, R.; Skolnick, M.; Sgaramella, V.; Bhatnagar, S. K.; Fontana, P.; Gutin, A.; Van de Peer, Y.; Salamini, F.; Viola, R. A high quality draft consensus sequence of the genome of a heterozygous grapevine variety. *PLoS One* **2007**, *2* (12), e1326.
(46) Sarry, J.-E.; Sommerer, N.; Sauvage, F.-X.; Bergoin, A.; Rossignol, M.; Albanac, G.; Romieu, C. Grape berry biochemistry revisited upon proteomic analysis of the mesocarp. *Proteomics* **2004**, *4*, 201–215.
(47) Sarry, J.-E.; Romieu, C. Personal communication.

(48) Ortega-García, F.; Blanco, S.; Ángeles Peinado, M.; Peragón, J. Polyphenol oxidase and its relationship with oleuropein concentration in fruits and leaves of olive (*Olea europaea*) cv. 'Picual' trees during fruit ripening. *Tree Physiol*. **2008**, *28*, 45–54.
(49) Damborský, J.; Petřek, M.; Banáš, P.; Otyepka, M. Identification of tunnels in proteins, nucleic acids, inorganic materials and molecular ensembles. *Biotechnol. J*. **2007**, *2*, 62–67.
(50) Söderhäll, I. Properties of carrot polyphenoloxidase. *Phytochemistry* **1995**, *39* (1), 33–38.
(51) Wood, B.; Ingraham, L. Labelled tyrosinase from labelled substrate. *Nature* **1965**, *205*, 291–292.
(52) Su, C.-C.; Hwang, T.-T.; Wang, O. Y.-P. Bonding in copper(II) imidazole complexes. *Transition Met. Chem*. **1992**, *17*, 91–96.
(53) Cuff, M.; Miller, K.; vanHolde, K.; Hendrickson, W. Crystal structure of a functional unit from Octopus hemocyanin. *J. Mol. Biol*. **1998**, *278* (4), 855–870.
(54) Robinson, S.; Dry, I. Broad bean leaf polyphenol oxidase is a 60-kilodalton protein susceptible to proteolytic cleavage. *Plant Physiol*. **1992**, *99*, 317–323.
(55) Wooten, J.; Federhen, S. Analysis of compositionally biased regions in sequence databases. *Methods Enzymol*. **1996**, *266*, 554–571.
(56) Hulo, N.; Bairoch, A.; Bulliard, V.; Cerutti, L.; Cuche, B.; De Castro, E.; Lachaize, C.; Langendijk-Genevaux, P. S.; Sigrist, C. J. A. The 20 years of PROSITE. *Nucleic Acids Res*. **2008**, *36*, D245–249.
(57) Trebst, A.; Depka, B. Polyphenol oxidase and photosynthesis research. *Photosynth. Res*. **1995**, *46*, 41–44.

Received for review August 20, 2009. Revised manuscript received December 7, 2009. Accepted December 8, 2009. A.M acknowledges the financial support from CONACYT Project No. 91999 and DGAPA-UNAM for supporting travel expenses for sabbatical time at the University of Cambridge (U.K.). V.M.V. was supported by a Fulbright Fellowship (1990−1994). We also acknowledge the BNL-NSLS in the USA for the support of the X-ray data collection at Brookhaven National Laboratories (USA).